

S-wave Superconductivity due to Orbital and Spin fluctuations in Fe-pnictides: Self-Consistent Vertex Correction with Self-Energy (SC-VC $_{\Sigma}$) Analysis

Seiichiro ONARI¹, Hiroshi KONTANI², Sergey V. Borisenko³, Volodymyr B. Zabolotnyy³ and Bernd Büchner³

¹ Department of Applied Physics, Nagoya University, Furo-cho, Nagoya 464-8603, Japan.

² Department of Physics, Nagoya University, Furo-cho, Nagoya 464-8602, Japan.

³ Leibniz-Institute for Solid State Research, IFW-Dresden, D-01171 Dresden, Germany

(Dated: November 9, 2018)

To understand the amazing variety of the superconducting states of Fe-based superconductors, we analyze the multiorbital Hubbard models for LaFeAsO and LiFeAs going beyond the random-phase approximation (RPA), by calculating the vertex correction (VC) and self-energy correction. Due to the spin+orbital mode coupling described by the VC, both orbital and spin fluctuations mutually develop, consistently with the experimental phase diagram with the orbital and magnetic orders. Due to both fluctuations, the s -wave gap function with sign-reversal (s_{\pm} -wave), without sign-reversal (s_{++} -wave), and nodal s -wave states are obtained, compatible with the experimental wide variety of the gap structure. Thus, the present theory provides a microscopic derivation of the normal and superconducting phase diagram based on the realistic Hubbard model.

PACS numbers: 74.70.Xa, 74.20.-z, 74.20.Rp

One of the main characteristic feature of Fe-based superconductors is their amazing variety of the superconducting gap structure. For example, isotropic fully-gapped s -wave state is realized in optimally-doped Co-doped and K-doped BaFe₂As₂ [1–3], while nodal s -wave states are expected in under and over-doped compounds [4]. In optimally P-doped BaFe₂As₂, in contrast, nodal s -wave state is observed by angle-resolved thermal conductivity [5] and angle-resolved photoemission spectroscopy (ARPES) [6–8]. Such variety of the gap structure would indicate the presence of competing pairing interactions in Fe-based superconductors [9–11].

To clarify the pairing mechanism in strongly correlated systems, its normal state phase diagram should be understood. The coincidence of the structure (or orbital) and magnetic quantum critical points (QCPs) indicates the coexistence of orbital and spin fluctuations in Fe-based superconductors. The large softening of the shear modulus C_{66} above the structure transition temperature T_S is a direct evidence of orbital fluctuations [12–17], and the orbital order or polarization had been observed in various compounds by polarized ARPES measurements [18, 19]. As for the superconductivity, the s -wave state with (without) sign reversal is caused by spin (orbital) fluctuations [20–26]. In BaFe₂(As,P)₂, the absence of the horizontal node on the hole-doped Fermi surface (h-FS) with $3z^2 - r^2$ -orbital character [6, 7] indicated the importance of the orbital fluctuations [9], and the loop-nodes on the electron-type Fermi surfaces (e-FSs) [5–7] can be explained by the competition between different spin fluctuations [10, 11] or that between spin and orbital fluctuations [9].

The normal state phase diagram with *non-magnetic* structure transition cannot be explained by the random-phase-approximation (RPA) based on the multiorbital Hubbard model. However, it can be explained by considering the vertex correction (VC), since the spin fluctuations induce the charge quadrupole order ($O_{x^2-y^2} \equiv$

$n_{xz} - n_{yz} \neq 0$) owing to the spin+orbital mode coupling described by the VC. This mechanism has been demonstrated by the diagrammatic [26, 27] as well as the renormalization group [28] methods in several multiorbital models. Similar spin-orbital coupling beyond the RPA had also been discussed in Refs. [29, 30]. We stress that spin fluctuations could also induce the spin quadrupole ($\phi = \mathbf{s}_A \cdot \mathbf{s}_B$) if $J_1 \sim 2J_2$ is realized [12], so the correct quadrupole order should be elucidated experimentally. The strain-quadrupole order coupling derived from the fitting of C_{66} is very large, which would be natural for the charge quadrupole scenario [13]. Now, the next significant challenge is to elucidate the pairing mechanism of the Fe-based superconductors by taking the VC into account.

In this paper, we develop a theory beyond the RPA, by calculating both the VC and the self-energy Σ self-consistently. By this “self-consistent VC+ Σ (SC-VC $_{\Sigma}$) method”, we obtain the mutual development of spin and orbital fluctuations. Therefore, both the s -wave state with sign change (s_{\pm} -wave) and that without sign change (s_{++} -wave), both of which are promising candidate pairing states, are naturally reproduced based on the two different realistic Hubbard models. No additional interactions such as the quadrupole interaction [24] were introduced to the models. The obtained smooth $s_{++} \leftrightarrow s_{\pm}$ crossover could explain the wide variety of gap structures in Fe-based superconductors.

In the following, we explain the SC-VC $_{\Sigma}$ method. First, we employ the five-orbital Hubbard model for LaFeAsO introduced in Ref. [20]. We denote d -orbitals $3z^2 - r^2$, xz , yz , xy , and $x^2 - y^2$ as 1, 2, 3, 4 and 5, respectively. Hereafter, x, y -axes are along the nearest Fe-Fe direction. The Fermi surfaces are mainly composed of orbitals 2, 3 and 4 [31]. The susceptibility for the charge (spin) channel is given by the following 25×25 matrix form in the orbital basis:

$$\hat{\chi}^{c(s)}(q) = \hat{\chi}^{\text{irr},c(s)}(q)(1 - \hat{\Gamma}^{c(s)}\hat{\chi}^{\text{irr},c(s)}(q))^{-1}, \quad (1)$$

where $q = (\mathbf{q}, \omega_l = 2\pi lT)$, and $\hat{\Gamma}^{c(s)}$ represents the Coulomb interaction for the charge (spin) channel composed of U , U' and J given in Refs. [24, 25, 32]. The irreducible susceptibility in Eq. (1) is given as

$$\hat{\chi}^{\text{irr},c(s)}(q) = \hat{\chi}^0(q) + \hat{X}^{c(s)}(q), \quad (2)$$

where $\chi_{ll',mm'}^0(q) = -T \sum_p G_{lm}(p+q)G_{m'l'}(p)$ is the bare bubble, and the second term is the VC, which is essential to produce the orbital fluctuations as discussed in Ref. [26]. In the SC-VC $_{\Sigma}$ method, Green's function \hat{G} is given by Dyson's equation $\hat{G} = (\hat{G}_0^{-1} - \hat{\Sigma})^{-1}$, where \hat{G}_0 is the bare Green's function and $\hat{\Sigma}$ is the self-energy. (In the SC-VC method, we put $\hat{\Sigma} = 0$.) In order to measure the distance from the criticality, we introduce the charge (spin) Stoner factor $\alpha_{\mathbf{q}}^{c(s)}$, which is the largest eigenvalue of $\hat{\Gamma}^{c(s)}\hat{\chi}^{\text{irr},c(s)}(\mathbf{q})$ at $\omega_l = 0$ [24]: The charge (spin) susceptibility diverges when $\alpha^{c(s)} \equiv \max_{\mathbf{q}}\{\alpha_{\mathbf{q}}^{c(s)}\} = 1$.

Here, we introduce VCs due to the Aslamazov-Larkin (AL) terms, which is the second order term with respect to $\hat{\chi}^{c,s}$ and becomes important near the QCP [26, 33]. The VCs for charge (spin) sector are denoted as $\hat{X}^{c(s)}(q) \equiv \hat{X}^{\uparrow,\uparrow}(q) + (-)\hat{X}^{\uparrow,\downarrow}(q)$. The AL term for the charge sector, $X_{ll',mm'}^{\text{AL},c}(q)$, is given as

$$\begin{aligned} \frac{T}{2} \sum_k \sum_{a \sim h} \Lambda_{ll',ab,ef}(q; k) \{V_{ab,cd}^c(k+q)V_{ef,gh}^c(-k) \\ + 3V_{ab,cd}^s(k+q)V_{ef,gh}^s(-k)\} \Lambda'_{mm',cd,gh}(q; k), \quad (3) \end{aligned}$$

where $\hat{V}^{s,c}(q) \equiv \hat{\Gamma}^{s,c} + \hat{\Gamma}^{s,c}\hat{\chi}^{s,c}(q)\hat{\Gamma}^{s,c}$, $\hat{\Lambda}(q; k)$ and $\hat{\Lambda}'(q; k)$ are the three-point vertex made of three Green functions[26]. We include all U^2 -terms without the double counting to obtain reliable results. Note that we neglect $\hat{X}^{\text{AL},s}$ because the contribution of $\hat{X}^{\text{AL},s}$ is much smaller than that of $\hat{X}^{\text{AL},c}$ [26–28].

The 5×5 self-energy matrix $\hat{\Sigma}$ in the fluctuation-exchange (FLEX) approximation is given by

$$\Sigma_{lm}(k) = T \sum_q \sum_{l',m'} V_{ll',mm'}^{\Sigma}(q) G_{l'm'}(k-q), \quad (4)$$

where $\hat{V}^{\Sigma}(q)$ is the effective interaction for the self-energy: $\hat{V}^{\Sigma}(q) = \frac{3}{2}\hat{V}^s(q) + \frac{1}{2}\hat{V}^c(q) - \frac{1}{4}(\hat{\Gamma}^c - \hat{\Gamma}^s)\hat{\chi}^0(q)(\hat{\Gamma}^c - \hat{\Gamma}^s) - \hat{\Gamma}^b\hat{\chi}^0(q)\hat{\Gamma}^b$, where $\Gamma_{ll',mm'}^b = -U' + J$ for $l = l' \neq m = m'$ and $\Gamma_{ll',mm'}^b = 0$ for others. The third and fourth terms of right hand side in $\hat{V}^{\Sigma}(q)$ are required to cancel the double counting in the 2nd order diagrams. By solving above equations, we obtain the susceptibilities and self-energy self-consistently.

In our calculation, we neglect the Maki-Thompson (MT) terms since it is much smaller than the AL term as explained in Ref. [26]. The dominance of the AL term is also verified by recent renormalization group study [28]. We use \hat{G}_0 in calculating Λ and Λ' in Eq. (3) since they are underestimated at high temperatures ($T \sim 0.05$) due to large quasiparticle damping $\text{Im}\Sigma(\mathbf{q}, -i\delta) \propto T$.

We use 64×64 \mathbf{k} -meshes and 256 Matsubara frequencies at $T = 0.05$ eV, and set the unit of energy as eV. Hereafter, we put the constraint $U = U' + 2J$. The Fermi surfaces in the LaFeAsO model for $n = 6.1$ are shown in Fig. 1 (a), where θ is denoted by the azimuthal angle from k_x axis. Figure 1 (b), (c) and (d) shows the obtained $\chi_{22,22}^c(\mathbf{q})$, $\chi_{24,42}^c(\mathbf{q})$ and $\chi_{34,43}^c(\mathbf{q})$ for $J/U = 0.15$ and $U = 2.2$ ($\alpha_s = 0.96$ and $\alpha_c = 0.97$) using the SC-VC $_{\Sigma}$ method, respectively. The development of the ferro-orbital fluctuations explains the softening of the shear modulus C_{66} and structure transition, and both ferro- and antiferro (AF)-orbital fluctuations are the driving force of the s_{++} -wave state. Here, orbital fluctuations can develop for much large J/U compared to the SC-VC method [26], since the value of U for the ordered state increases due to the self-energy, and therefore $\hat{X}^{\text{AL},c} \propto U^4$ is enlarged. We verified that similar results are obtained for $6.0 \leq n \leq 6.1$, even if the h-FS at $(\pm\pi, \pm\pi)$ appears.

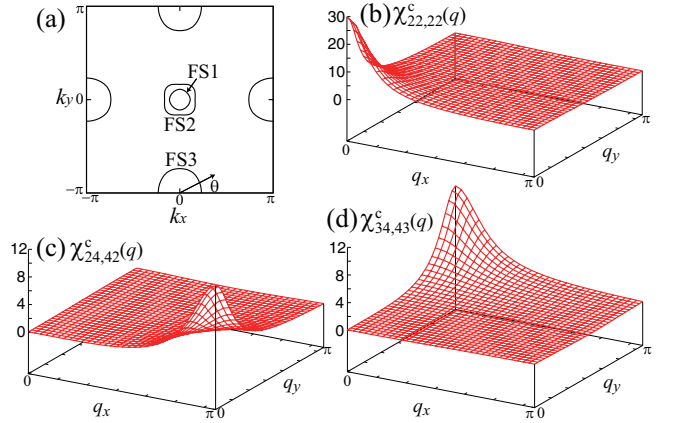


FIG. 1: (color online) (a) FSs of the LaFeAsO five-orbital model for $n = 6.1$, where θ is denoted by the azimuthal angle from k_x axis. (b) $\chi_{22,22}^c(\mathbf{q})$, (c) $\chi_{24,42}^c(\mathbf{q})$ and (d) $\chi_{34,43}^c(\mathbf{q})$ given by the SC-VC $_{\Sigma}$ method for $J/U = 0.15$, $\alpha^s = 0.96$, and $\alpha^c = 0.97$.

Next, we focus on the superconducting gap function. The linearized Eliashberg equation in the absence of impurities is given by

$$\begin{aligned} \lambda_E \phi_{ll'}(k) = - T \sum_{k', m_i} V_{lm_1, m_4 l'}^E(k-k') G_{m_1 m_2}(k') \\ \times \phi_{m_2 m_3}(k') G_{m_4 m_3}(-k') \quad (5) \end{aligned}$$

where $\phi_{ll'}(k)$ is the anomalous self-energy and λ_E is the eigenvalue that reaches unity at $T = T_c$. When T is fixed, λ_E is considered to be guide of stability of the superconductivity, *i.e.*, the larger eigenvalue λ_E corresponds to the higher T_c . The pairing interaction \hat{V}^E in Eq. (5) is

$$\hat{V}^E(q) = \frac{3}{2}\hat{\Gamma}^s\hat{\chi}^s(q)\hat{\Gamma}^s - \frac{1}{2}\hat{\Gamma}^c\hat{\chi}^c(q)\hat{\Gamma}^c + \hat{V}^{(1)}, \quad (6)$$

where $\hat{\chi}^{s,c}$ is given by the SC-VC $_{\Sigma}$ method for $n_{\text{imp}} = 0$, and $\hat{V}^{(1)}$ denotes the first order term. The first (second)

term in Eq. (6) works to set $\Delta_{\text{FS1},2} \cdot \Delta_{\text{FS3},4} < 0$ (> 0) [32].

Finally, we obtain a gap function $\hat{\Delta}(\mathbf{k}) = \hat{\phi}(\mathbf{k}, \omega_n = \pi T) / \hat{Z}(\mathbf{k})$ in the band representation, where mass enhancement factor \hat{Z} is given as $Z_\alpha(\mathbf{k}) = 1 - \frac{\text{Im}\Sigma_\alpha(\mathbf{k}, \omega_n = \pi T)}{\pi T}$ in a band α . We obtain $Z \sim 3$ in the present study. We note that the absolute value of Δ is not important since the Eliashberg Eq. (5) is linearized.

In Eq. (6), $\hat{V}^{(1)} = \frac{1}{2}\hat{\Gamma}^s - \frac{1}{2}\hat{\Gamma}^c$ represents the first-order terms with respect to the Coulomb interaction. This term gives the Anderson-Morel pseudopotential $\mu^* \approx UN(0)[1 + UN(0)\ln(W_{\text{band}}/\omega_0)]^{-1}$, where $N(0)$ is the density-of-states (DOS) at the Fermi level, W_{band} is the bandwidth, and ω_0 is the energy-scale of the orbital and spin fluctuations [34]: $\omega_0 \sim T$ is expected in optimally-doped compounds close to the orbital and magnetic QCPs. Although μ^* suppresses the s_{++} -wave state, we can expect that this term is approximately canceled out by the weak e-ph interaction $\lambda_{\text{e-ph}} (\sim 0.2)$.

Hereafter, we calculate the superconducting gap functions based on the gap equation in Eq. 6, by fixing the ratio J/U while choosing U so as to satisfy $\alpha_c = 0.97$. Figure 2 (a) and (b) show the obtained gap structures for $J/U = 0.1$ ($U = 2.0$; $\alpha_s = 0.91$) with $\hat{V}^{(1)}$ ($\lambda_E = 0.35$) and those without $\hat{V}^{(1)}$ ($\lambda_E = 0.51$), respectively. The dropping of $\hat{V}^{(1)}$ will be justified since we expect that μ^* is as small as $\lambda_{\text{e-ph}} (\sim 0.2)$ due to the retardation. In both cases, fully-gapped s_{++} -wave states are obtained. In (b), gap functions of FS1 and FS2 are as large as that of FS3 since $\hat{V}^{(1)}$ is repulsive interaction and unfavorable to the s_{++} -wave state. The s_{++} -wave state is derived from the strong developments of $\chi_{22,22}(q)$ and $\chi_{24,42}(q)$ shown in Fig.1.

Next, we move to $J/U = 0.12$, where the spin fluctuations are stronger than that for $J/U = 0.1$. Figure 2 (c) and (d) show the obtained gap structures for $J/U = 0.12$ ($U = 2.1$; $\alpha_s = 0.93$) with $\hat{V}^{(1)}$ ($\lambda_E = 0.49$) and those without $\hat{V}^{(1)}$ ($\lambda_E = 0.57$), respectively. In both (c) and (d), the obtained states are the nodal s -wave states which is intermediate between s_{++} -wave and s_{\pm} -wave states due to the competition between orbital and spin fluctuations. We note that the relation $J/U = 0.12 - 0.15$ is estimated by the first principle calculation [35].

We also study the impurity effect on the superconducting state, by introducing the impurity T -matrix into Eq. (5) according to Refs. [24, 36, 37]. Here, we discuss the impurity-induced $s_{\pm} \rightarrow s_{++}$ crossover for $J/U = 0.15$ ($U = 2.2$; $\alpha_s = 0.96$; $\lambda_E = 0.33$), in which the spin and orbital fluctuations are comparable. In the absence of impurities ($n_{\text{imp}} = 0$), the s_{\pm} -wave state is realized as shown in Fig. 3 (a). As increasing n_{imp} , the crossover between s_{++} -wave and s_{\pm} -wave states is expected, as discussed in Refs. [9, 24]. In fact, Fig. 3 (b) and (c) shows the obtained gap functions for $n_{\text{imp}} = 5\%$ and 10% , respectively, when the impurity potential is $I = 1\text{eV}$. Since the obtained $\lambda_E (\sim 0.33)$ is almost unchanged for $n_{\text{imp}} = 0 \sim 10\%$, the impurity-induced $s_{\pm} \rightarrow s_{++}$

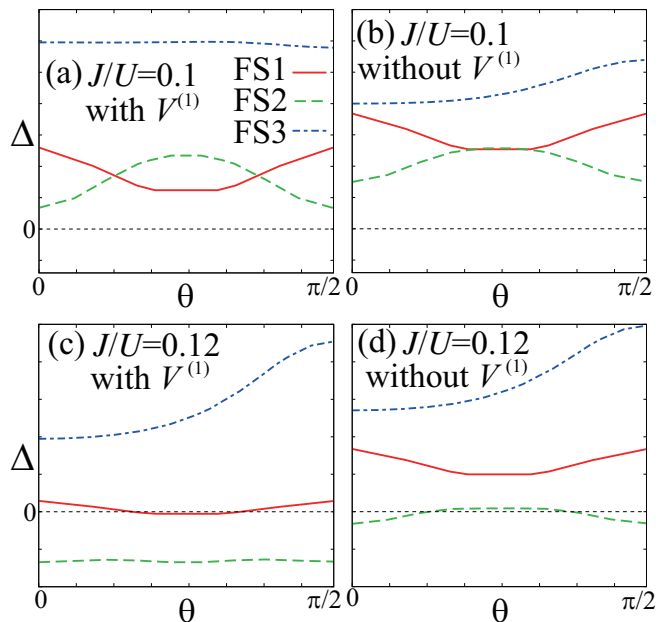


FIG. 2: (color online) (a) θ dependences of gap functions for $J/U = 0.1$ with $\hat{V}^{(1)}$ and (b) those without $\hat{V}^{(1)}$. (c) θ dependences of gap functions for $J/U = 0.12$ with $\hat{V}^{(1)}$ and (d) those without $\hat{V}^{(1)}$.

crossover will be realized with small change in T_c . Since the impurity concentration to realize the crossover is scaled with T , $n_{\text{imp}} = 10\%$ for $T = 0.05$ would correspond to $n_{\text{imp}} \sim 1\%$ for $T = T_c \sim 0.005$. Therefore, the s_{++} -wave state will be realized in various iron-based superconductors with finite randomness.

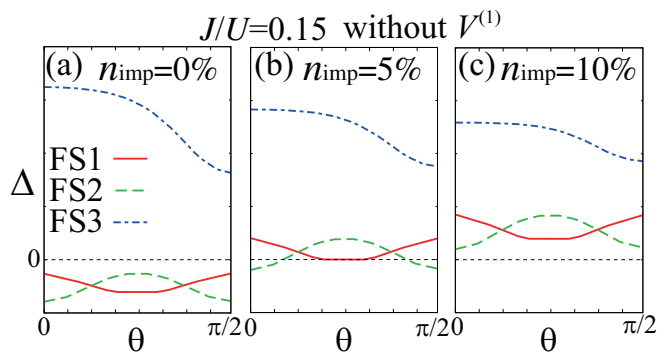


FIG. 3: (color online) (a) θ dependences of gap functions without $\hat{V}^{(1)}$ for $J/U = 0.15$ with $n_{\text{imp}} = 0\%$, (b) those with $n_{\text{imp}} = 5\%$, and (c) those with $n_{\text{imp}} = 10\%$.

In the following, we study the superconducting state of LiFeAs, using the tight-binding model given by fitted to the ARPES data of LiFeAs [38]. The FSs in the model are shown as Fig. 4 (a) for $n = 6.0$, in which the large d_{xy} -orbital h-FS4 around $\mathbf{k} = (\pi, \pi)$ is added to the model of LaFeAsO. Within the RPA, the s_{\pm} -wave state is favored by the h-FS4 [39]. However, as shown in Fig. 4 (b) and

(c) for $J/U = 0.12$, $U = 1.2$ at $T = 0.03$ ($\alpha_s = 0.92$ and $\alpha_c = 0.97$), the AF-spin and AF-orbital fluctuations are strongly enhanced in the SC-VC $_{\Sigma}$ method. In contrast, the ferro-orbital fluctuations are relatively small, consistently with the absence of the structure transition in LiFeAs. The gaps obtained for $J/U = 0.12$, $n_{\text{imp}} = 0\%$ at $T = 0.03$ are s_{++} -wave mediated by the AF-orbital fluctuation as shown in Fig. 4 (d) with $\hat{V}^{(1)}$ ($\lambda_E = 0.40$) and (e) without $\hat{V}^{(1)}$ ($\lambda_E = 0.53$). Thus, the fully-gapped s_{++} -wave state is realized for $J/U = 0.12$ even for $n_{\text{imp}} = 0$.

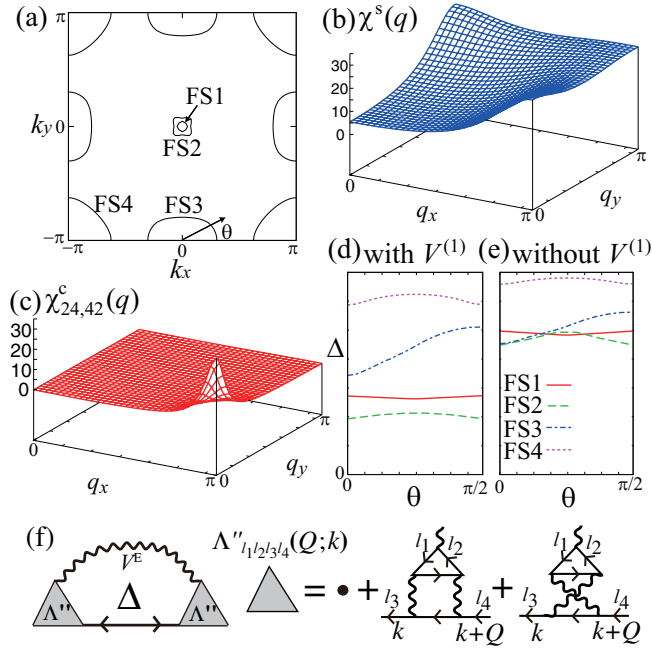


FIG. 4: (color online) (a) FSs of the LiFeAs model for $n = 6.0$. (b) $\chi^s(\mathbf{q}) = \sum_{l,m} \chi_{ll,mm}^s(\mathbf{q})$, (c) $\chi_{24,42}^c(\mathbf{q})$ given by SC-VC $_{\Sigma}$ method in the LiFeAs model for $J/U = 0.12$, $\alpha^s = 0.92$, and $\alpha^c = 0.97$ at $T = 0.03$. (d) θ dependences of gap functions for $J/U = 0.12$, $n_{\text{imp}} = 0\%$ at $T = 0.03$ with $\hat{V}^{(1)}$, and (e) those without $\hat{V}^{(1)}$. (f) Feynman diagram of $\hat{\Delta}$ and VC $\hat{\Lambda}''$ for the charge sector \hat{V}^c in the pairing interaction \hat{V}^E .

Here, the calculation temperature is much higher than T_c since the SC-VC $_{\Sigma}$ method is heavy numerical calculation. For this reason, the obtained gap is nearly isotropic on each FS. It is our important future problem to study the experimental large gap anisotropy at much lower temperatures.

In the present study, we dropped the VC for the electron-boson coupling constant in the gap equation, shown by $\hat{\Lambda}''(q; k)$ in Fig. 4 (f). Recently, we had verified that $|\hat{\Lambda}''(q; k)|$ due to the AL type diagram in Fig. 4 (f) is much larger than unity for the charge sector [40]. This fact means the violation of the Migdal's theorem. Then, λ_E for the s_{++} -wave state is enlarged since the charge pairing interaction $\frac{1}{2}\hat{\Gamma}^c\hat{\chi}^c(q)\hat{\Gamma}^c$, given by the second term in Eq. (6), is multiplied by $|\hat{\Lambda}''(q; k)|^2$. Therefore, the s_{++} -wave state is further stabilized by the VC for the electron-orbital coupling, going beyond the Eliashberg theory.

In summary, we have studied the normal and superconducting states of LaFeAsO and LiFeAs using the SC-VC $_{\Sigma}$ theory. We obtain both the s_{++} - and s_{\pm} -wave gap, both of which are promising candidate pairing states, based on two very different but realistic tight-binding Hubbard models with $J/U \lesssim 0.15$. No additional interactions such as the quadrupole interaction were introduced. We stress that a smooth $s_{++} \leftrightarrow s_{\pm}$ crossover could be realized by introducing the impurities or magnetic ordered state, consistently with the robustness of T_c [41–44] and the wide variety of gap structures in Fe-based superconductors.

Acknowledgments

We are grateful to A. Chubukov, P.J. Hirschfeld, J. Schmalian and R. Fernandes for useful discussions. This study has been supported by Grants-in-Aid for Scientific Research from MEXT of Japan. Part of numerical calculations were performed on the Yukawa Institute Computer Facility.

-
- [1] K. Hashimoto, T. Shibauchi, T. Kato, K. Ikada, R. Okazaki, H. Shishido, M. Ishikado, H. Kito, A. Iyo, H. Eisaki, S. Shamoto and Y. Matsuda, Phys. Rev. Lett. **102**, 017002 (2009).
- [2] H. Ding, P. Richard, K. Nakayama, K. Sugawara, T. Arakane, Y. Sekiba, A. Takayama, S. Souma, T. Sato, T. Takahashi, Z. Wang, X. Dai, Z. Fang, G. F. Chen, J. L. Luo and N. L. Wang, Europhys. Lett. **83**, 47001 (2008).
- [3] T. Shimojima, F. Sakaguchi, K. Ishizaka, Y. Ishida, T. Kiss, M. Okawa, T. Togashi, C.-T. Chen, S. Watanabe, M. Arita, K. Shimada, H. Namatame, M. Taniguchi, K. Ohgushi, S. Kasahara, T. Terashima, T. Shibauchi, Y. Matsuda, A. Chainani, and S. Shin, Science **332**, 564 (2011).
- [4] M. A. Tanatar, J.-Ph. Reid, H. Shakeripour, X. G. Luo, N. Doiron-Leyraud, N. Ni, S. L. Budko, P. C. Canfield, R. Prozorov and L. Taillefer, Phys. Rev. Lett. **104**, 067002 (2010).
- [5] M. Yamashita, Y. Senshu, T. Shibauchi, S. Kasahara, K. Hashimoto, D. Watanabe, H. Ikeda, T. Terashima, I. Vekhter, A. B. Vorontsov, and Y. Matsuda, Phys. Rev. B **84**, 060507(R) (2011).
- [6] T. Shimojima *et al.*, Solid State Commun. **152**, 695 (2012).
- [7] T. Yoshida *et al.*, arXiv:1301.4818.
- [8] Y. Zhang *et al.*, Nature phys. **8**, 371 (2012).
- [9] T. Saito, S. Onari, and H. Kontani, Phys. Rev. B **87**

- 045115 (2013); In the tight-binding model for BaFe_2As_2 , the nodal structure appears on the e-FSs during the $s_{++} \leftrightarrow s_{\pm}$ crossover.
- [10] S. Maiti *et al.*, Phys. Rev. B **84**, 224505 (2011).
- [11] M. Khodas and A. V. Chubukov, Phys. Rev. B **86**, 144519 (2012).
- [12] R.M. Fernandes, L. H. VanBebber, S. Bhattacharya, P. Chandra, V. Keppens, D. Mandrus, M.A. McGuire, B.C. Sales, A.S. Sefat and J. Schmalian, Phys. Rev. Lett. **105**, 157003 (2010).
- [13] H. Kontani, Y. Inoue, T. Saito, Y. Yamakawa, and S. Onari, Solid State Communications, **152** (2012) 718.
- [14] M. Yoshizawa, R. Kamiya, R. Onodera, Y. Nakanishi, K. Kihou, H. Eisaki and C. H. Lee, Phys. Soc. Jpn. **81**, 024604 (2012).
- [15] T. Goto, R. Kurihara, K. Araki, K. Mitsumoto, M. Akatsu, Y. Nemoto, S. Tatematsu and M. Sato, J. Phys. Soc. Jpn. **80**, 073702 (2011).
- [16] A. E. Bohmer, P. Burger, F. Hardy, T. Wolf, P. Schweiss, R. Fromknecht, M. Reinecker, W. Schranz, and C. Meingast, arXiv:1305.3515.
- [17] Y. Gallais, R. M. Fernandes, I. Paul, L. Chauviere, Y.-X. Yang, M.-A. Measson, M. Cazayous, A. Sacuto, D. Colson, and A. Forget, arXiv:1302.6255
- [18] M. Yi, D. H. Lu, J.-H. Chu, J.G. Analytis, A.P. Sorini, A. F. Kemper, S.-K. Mo, R.G. Moore, M. Hashimoto, W.S. Lee, Z. Hussain, T.P. Devereaux, I.R. Fisher and Z.-X. Shen, Proc. Natl. Acad. Sci. U.S.A. **108**, 6878.
- [19] T. Shimojima *et al.*, arXiv:1305.3875
- [20] K. Kuroki, S. Onari, R. Arita, H. Usui, Y. Tanaka, H. Kontani and H. Aoki, Phys. Rev. Lett. **101**, 087004 (2008).
- [21] I. I. Mazin, D. J. Singh, M.D. Johannes, and M. H. Du, Phys. Rev. Lett. **101**, 057003 (2008).
- [22] P.J. Hirschfeld, M.M. Korshunov and I.I. Mazin, Rep. Prog. Phys. **74**, 124508 (2011).
- [23] A. V. Chubukov, Annu. Rev. Condens. Matter Phys. **3**, 57 (2012).
- [24] H. Kontani and S. Onari, Phys. Rev. Lett. **104**, 157001 (2010).
- [25] T. Saito *et al.* Phys. Rev. B **82**, 144510 (2010).
- [26] S. Onari and H. Kontani, Phys. Rev. Lett. **109**, 137001 (2012).
- [27] Y. Ohno, M. Tsuchiizu, S. Onari, and H. Kontani, J. Phys. Soc. Jpn. **82**, 013707 (2013).
- [28] M. Tsuchiizu, Y. Ohno, S. Onari, and H. Kontani, Phys. Rev. Lett. **111** (2013). (arXiv:1209.3664)
- [29] S. Liang, A. Moreo, and E. Dagotto, arXiv:1305.1879
- [30] F. Kruger *et al.*, Phys. Rev. B **79** (2009) 054504.
- [31] H. Kontani, T. Saito and S. Onari, Phys. Rev. B **84**, 024528 (2011).
- [32] T. Takimoto, T. Hotta, T. Maehira and K. Ueda, J. Phys. Condens. Matter **14**, L369 (2002).
- [33] T. Moriya, *Spin Fluctuations in Itinerant Electron Magnetism* (Springer-Verlag, 1985); A. Kawabata: J. Phys. F **4**, 1477 (1974).
- [34] P. Morel and P. W. Anderson, Phys. Rev. **125**, 1263 (1962).
- [35] T. Miyake, K. Nakamura, R. Arita and M. Imada, J. Phys. Soc. Jpn. **79**, 044705 (2010).
- [36] S. Onari and H. Kontani, Phys. Rev. Lett. **103** 177001 (2009).
- [37] Y. Yamakawa, S. Onari, and H. Kontani, Phys. Rev. B **87** 195121 (2013).
- [38] S.V. Borisenko, V.B. Zabolotnyy, A.A. Kordyuk, D.V. Evtushinsky, T.K. Kim, I.V. Morozov, R. Follath and B. Buchner, Symmetry **4**, 251 (2012).
- [39] K. Kuroki, H. Usui, S. Onari, R. Arita, H. Aoki, Phys. Rev. B **79**, 224511 (2009).
- [40] S. Onari and H. Kontani, unpublished.
- [41] A. Kawabata, S. C. Lee, T. Moyoshi, Y. Kobayashi and M. Sato, J. Phys. Soc. Jpn. **77**, 103704 (2008); M. Sato, Y. Kobayashi, S. C. Lee, H. Takahashi, E. Satomi and Y. Miura, J. Phys. Soc. Jpn. **79**, 014710 (2009); S.C. Lee, E. Satomi, Y. Kobayashi, and M. Sato, J. Phys. Soc. Jpn. **79**, 023702 (2010).
- [42] C. Tarantini, M. Putti, A. Gurevich, Y. Shen, R. K. Singh, J. M. Rowell, N. Newman, D. C. Larbalestier, P. Cheng, Y. Jia, and H.-H. Wen, Phys. Rev. Lett. **104**, 087002 (2010).
- [43] Y. Nakajima, T. Taen, Y. Tsuchiya, T. Tamegai, H. Kitamura, and T. Murakami, arXiv:1009.2848.
- [44] Y. Li, J. Tong, Q. Tao, C. Feng, G. Cao, W. Chen, F.C. Zhang, and Z.A. Xu, New J. Phys. **12** (2010) 083008.